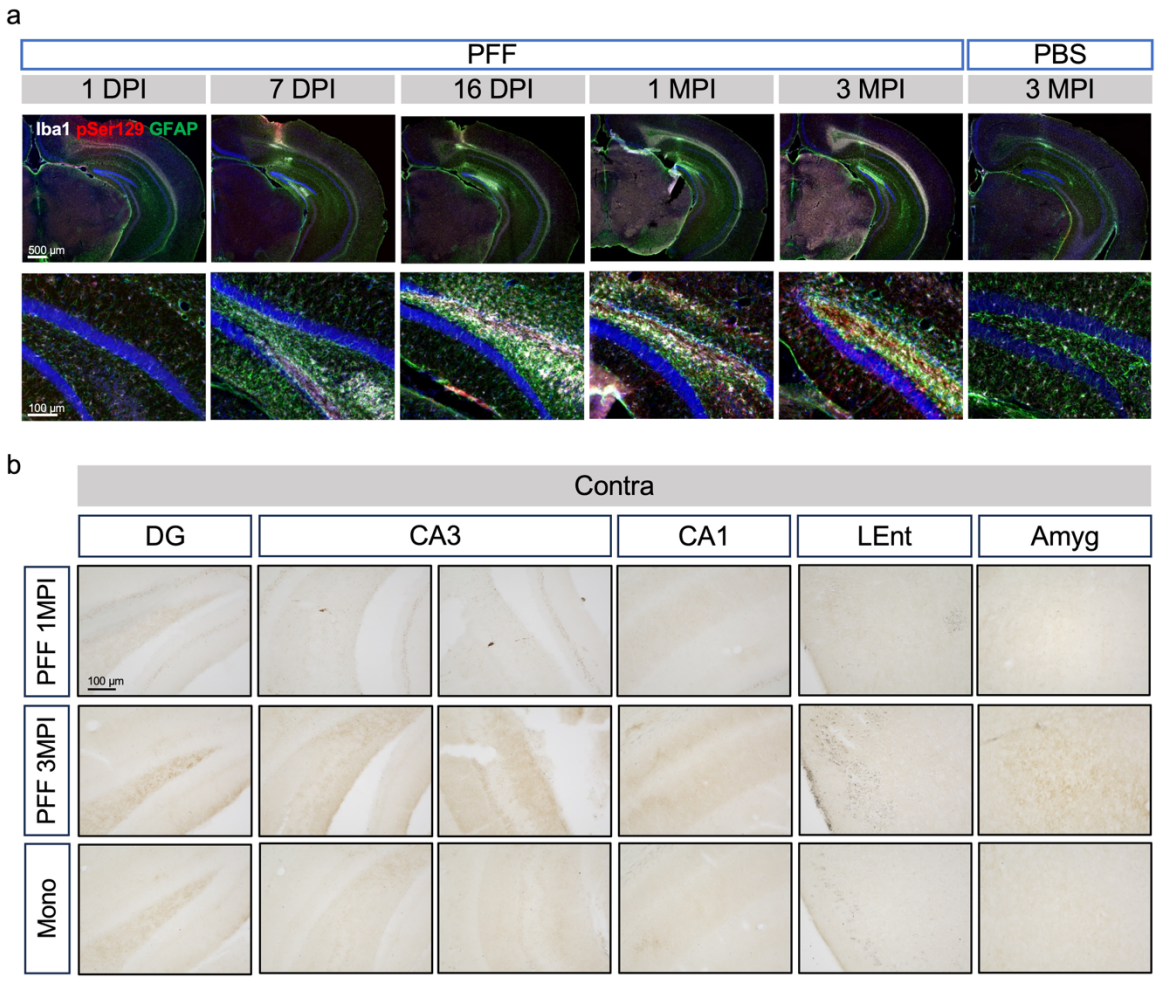
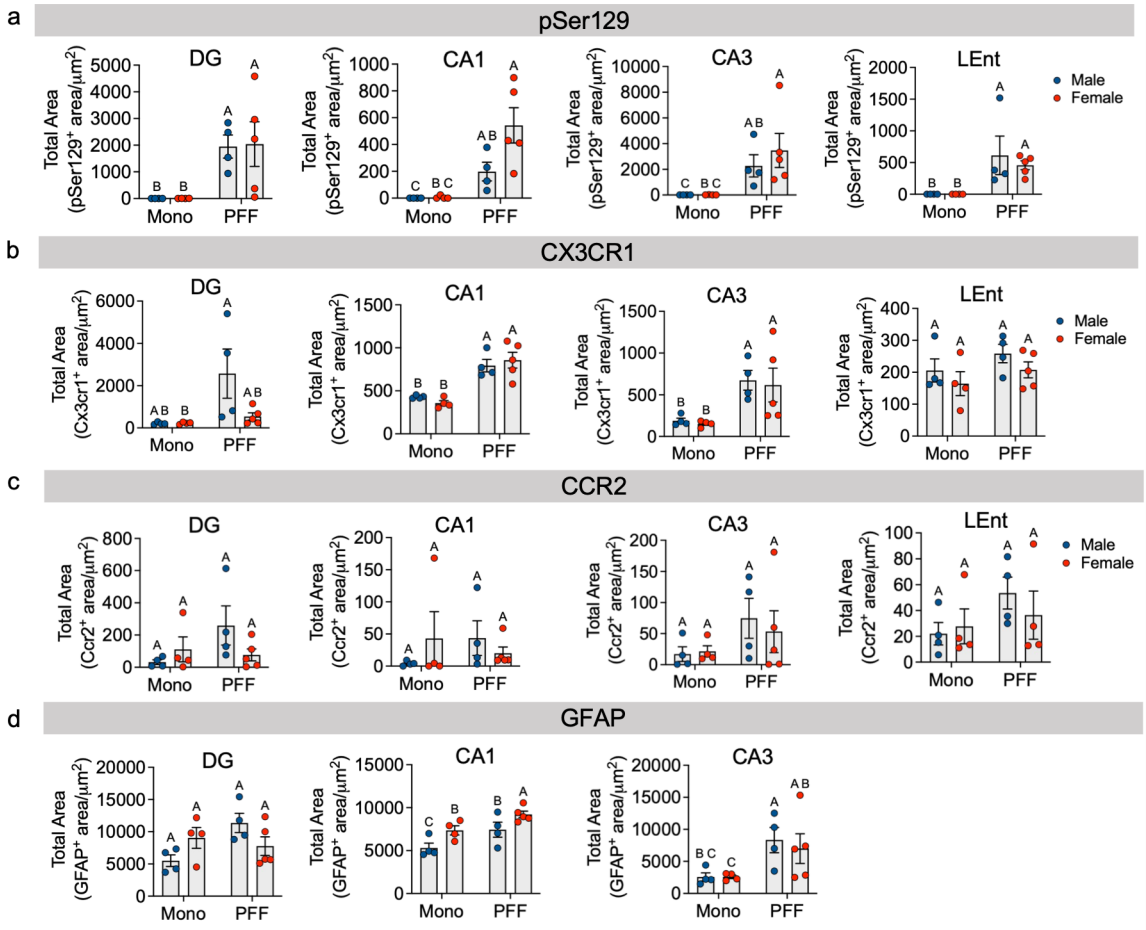
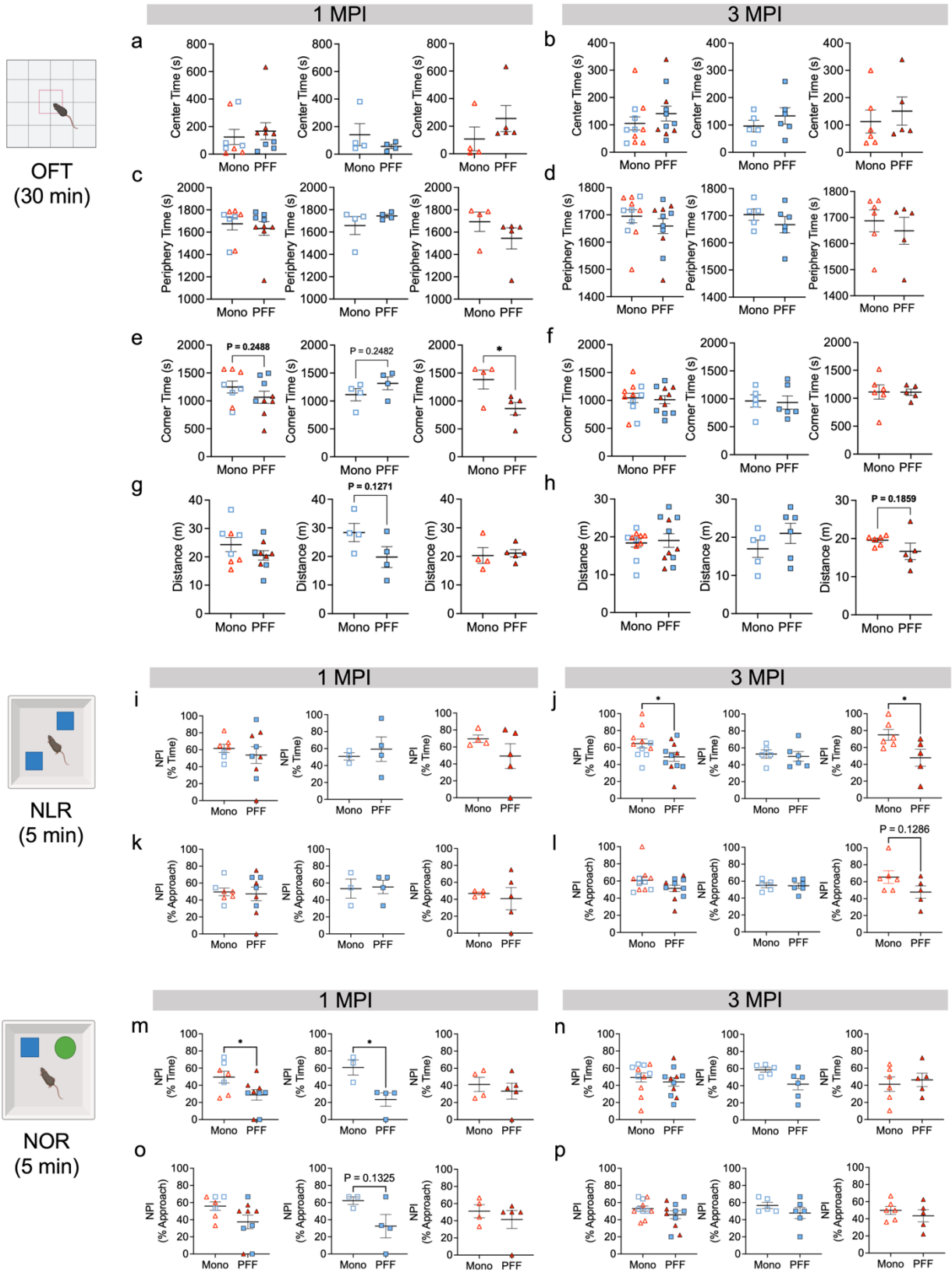
Supplementary figures



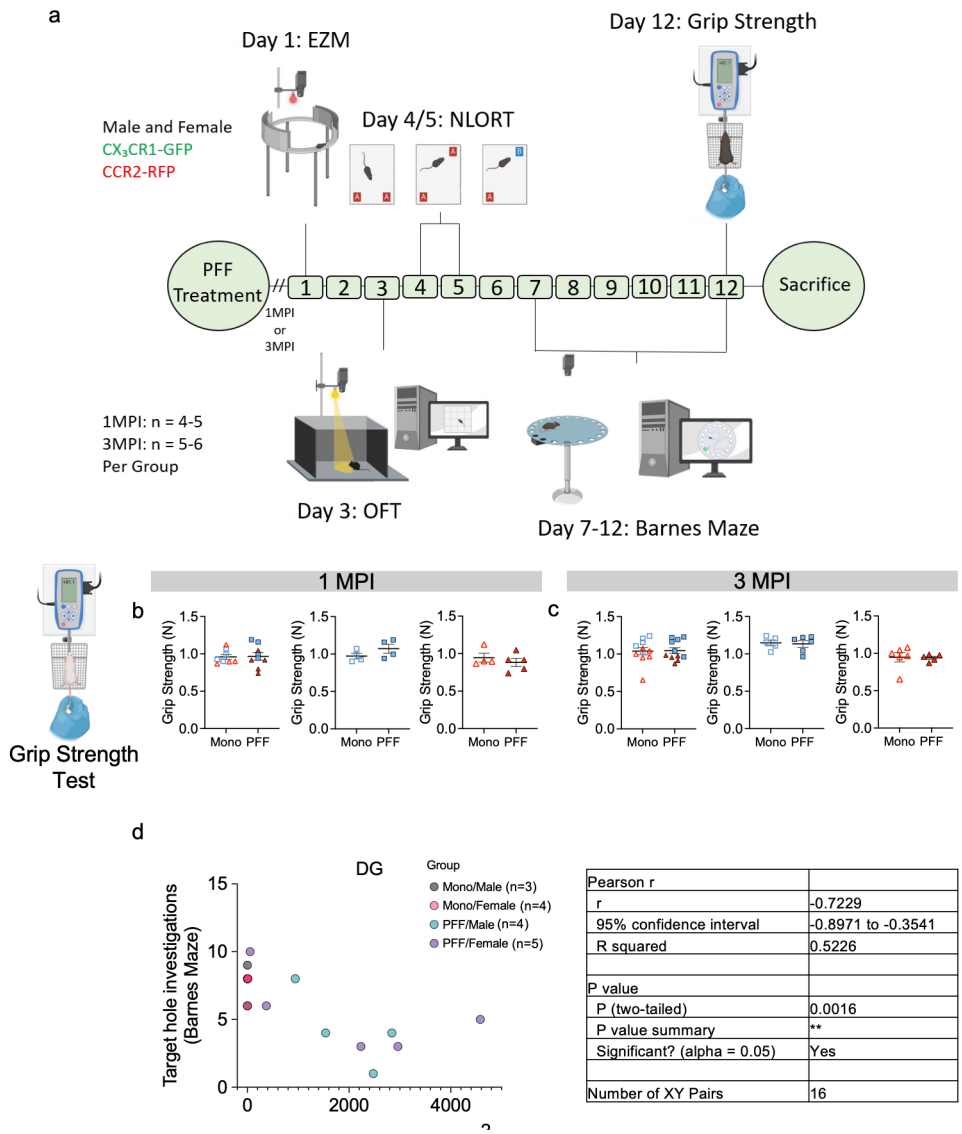
Supplementary Fig. 1 Temporal and contralateral patterns of α-syn pathology following hippocampal injection. **a**) Representative images of the mouse hippocampus, immunostained with Iba1 (white), pSer129 (red), and GFAP (green) at 1-, 7-, 16-days post-injection (DPI), and 1- and 3-months post-injection (MPI) after injection with either α-syn PFF or PBS. Scale bars = 500 µm or 100 µm. **b**) Representative images of the contralateral side of mouse hippocampus subsets (DG, CA1, and CA3), lateral entorhinal cortex (LEnt), and amygdala (Amyg), treated with proteinase K and immunostained with pSer129, at 1 and 3MPI. Scale bars = 100 µm.



Supplementary Fig. 2 Sex-associated differences in CA1 GFAP$^+$ area following bilateral PFF injection in *Cx3cr1*^{GFP}/*Ccr2*^{RFP} mice. a-d) Quantification of the total area occupied by **a**) pSer129$^+$, **b**) CX3CR1^{GFP}, **c**) CCR2^{RFP}, and **d**) GFAP$^+$ Inclusions per region of interest in the DG, CA1, CA3, and LEnt. Error bars represent ±SEM. Statistical comparisons were performed using two-way ANOVA with treatment and sex as factors, followed by Fisher's LSD test. Groups with no letters in common differ significantly ($P < 0.05$).


1 MPI
3 MPI
OFT
(30 min)
NLR
(5 min)
NOR
(5 min)
a
b
c
d
e
f
g
h
i
j
k
l
m
n
o
p
Center Time (s)
Periphery Time (s)
Corner Time (s)
Distance (m)
NPI (% Time)
NPI (% Approach)
Mono
PFF
P = 0.2488
P = 0.2482
*
P = 0.1271
P = 0.1859
P = 0.1286
P = 0.1325

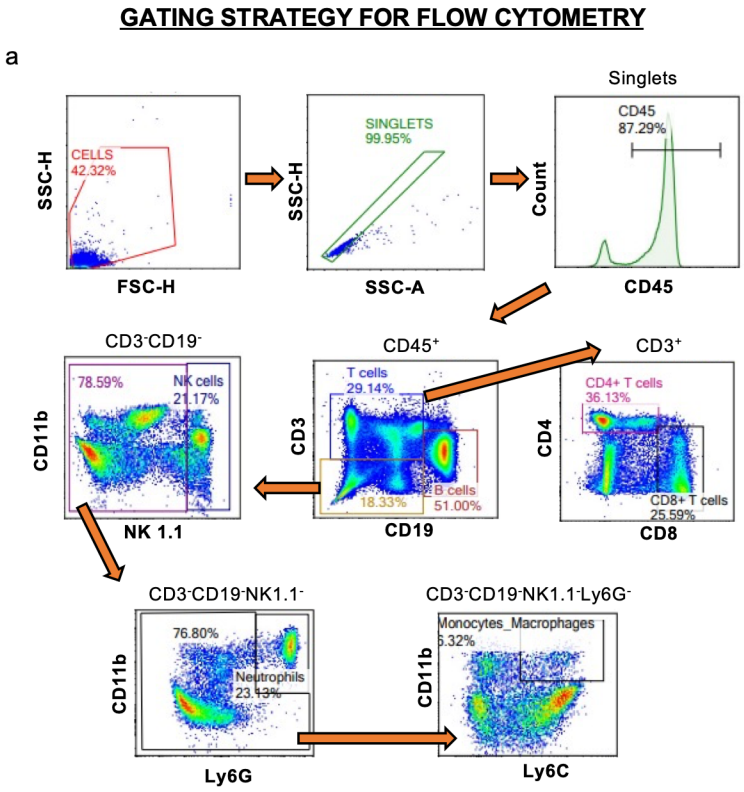
Supplementary Fig. 3 Open field behavior and novel location and novel object recognition following hippocampal α-syn injection. a, b) Center time on the OFT at 1MPI and at 3MPI, respectively. **c, d**) Periphery time on the OFT at 1MPI and at 3MPI, respectively. **e, f**) Corner time on the OFT at 1MPI and at 3MPI, respectively. **g, h**) Distance travelled on the OFT at 1MPI and at 3MPI, respectively. **i, j**) Novelty preference index (%) by time during 5 min of the NLRT at 1MPI and at 3 MPI. **k, l**) Novelty preference index (%) by approach during 5 min of the NLRT at 1MPI and at 3MPI, respectively. **m, n**) Novelty preference index (%) by time during 5 min of the NORT at 1MPI and at 3MPI, respectively. **o, p**) Novelty preference index (%) by approach during 5 min of the NORT at 1MPI and at 3 MPI. Error bars represent ± SEM. Statistical analyses were performed using an unpaired Student's t-test. $*P < 0.05$, $**P < 0.01$, $***P < 0.001$.



Pearson r	
r	-0.7229
95% confidence interval	-0.8971 to -0.3541
R squared	0.5226
P value	
P (two-tailed)	0.0016
P value summary	**
Significant? (alpha = 0.05)	Yes
Number of XY Pairs	16

Supplementary Fig. 4 Behavioral assessment timeline, grip strength, and the relationship between DG α-syn pathology and Barnes maze performance. a) Schematic of the behavioral assessment timeline. **b**) Forelimb grip strength (N) at 1MPI. **c**) Forelimb grip strength (N) at 3MPI. Error bars represent ± SEM. Statistical analyses were performed using an unpaired student's t-test. *p < 0.05, **p < 0.01, ***p < 0.001. **d**) Correlation between pSer129^{+} α-syn area in the DG and the number of target hole investigations during the Barnes maze probe trial at 1MPI. Pearson's

correlation included monomer- and PFF-injected males and females (r = -0.7229, p = 0.0016; n = 16).



Supplementary Fig. 5 Gating strategy for flow cytometric analysis of peripheral immune cells. a) Representative gating strategy used to identify leukocyte populations in the spleen, lymph nodes, and blood. Debris was excluded using forward and side scatter, followed by singlet selection to exclude doublets. $CD45^+$ leukocytes were then identified within the singlet population. CD3 and CD19 were used to identify T cells and B cells, respectively, and $CD3^-CD19^-$ cells were selected for further analysis. $CD3^+$ T cells were subdivided into $CD4^+$ and $CD8^+$ populations. Within the $CD3^-CD19^-$ population, NK cells were identified using NK 1.1 expression in conjunction with CD11b. $CD11b^+Ly6G^+$ neutrophils were identified within the non-NK

population, followed by identification of $CD11b^{+}Ly6C^{+}$ monocytes/macrophages within the remaining non-neutrophil population.